Magnetism of Fe/Pd superlattices

Ahmed Boufelfel and Roy M. Emrick
Department of Physics, The University of Arizona, Tucson, Arizona 85721

Charles M. Falco
Department of Physics and Optical Sciences Center and in the Arizona Research Laboratories, The University of Arizona, Tucson, Arizona 85721

(Received 6 December 1990)

A series of Fe/Pd superlattices of varying numbers of atoms per layer were fabricated. Structural properties were characterized by x-ray diffraction. Magnetic properties were studied by Mössbauer spectroscopy and transport properties by electrical-conductivity measurements. All properties studied could be explained by structural characteristics, such as grain size and interdiffusion, without the need of invoking superlattice effects.

I. INTRODUCTION

Metallic multilayers, where at least one of the layers is magnetic, have received considerable attention in recent years. Originally, one major interest was in interface magnetism,[1,2] where multiple layers were required simply to raise the signal to a satisfactory level. Many advances have been made since and high-quality superlattices of various metal-metal combinations now can be made somewhat routinely.[3]

Great strides also have been made on the theoretical scene. Freeman *et al.*[4,5] have made calculations of the surface magnetism in iron for both free and Ag(100) interfaces. Their results indicate that, at the free surface, the electrons become more free-atom-like and the magnetization increases, whereas the presence of a silver coating reduces the increase in magnetization. The relation between the local magnetic moment and the resulting hyperfine field $H_{\rm hf}$ at the given nucleus is greatly complicated at an interface. In the bulk, for pure metals, the two are proportional. However, at surfaces, conduction-electron polarization and dipole effects require a detailed treatment of each individual situation.[1,6]

Mössbauer spectroscopy has proved to be a useful tool in investigating these surface and interface effects because of the atomic nature of this probe.[7,8] That is, the Mössbauer effect provides information about the local environment rather than averages over the entire sample. Thus, it is ideally suited for determining $H_{\rm hf}$ both in the interior of a layer and at the surface. Because it is ferromagnetic and because it is the simplest Mössbauer isotope to use, iron is the obvious choice for one of the superlattice pairs.

It has been found that, for iron, the bulk hyperfine field establishes itself within a few atomic layers of the interface.[9] The hyperfine field of the material within the final few atomic layers may be greater or less than the bulk value, depending on the nature of the metal used for the other layer of the superlattice pair.[10] Because it is "nearly magnetic," Pd is an obvious candidate for superlattice studies. Hosoito *et al.*[11] performed a depth-sensitive Mössbauer study of Pd-Fe-Pd sandwiches and reported an anomalous behavior of the Fe layer at the interface with Pd. At 4.2 K they found $H_{\rm hf}$ was reduced from bulk and that, at 300 K, about 30% of the layer was paramagnetic.

At room temperature, bulk Fe is in the bcc phase with lattice constant $a=2.86$ Å and Pd is fcc with $a=3.88$ Å. These materials typically grow with their densest packed layers in the plane of the sample, so that the resulting interfaces in the multilayer are between Fe$\{110\}$ and the Pd$\{111\}$ planes. The (anisotropic) lattice constant mismatch is 4.3% along the Fe $\langle 100 \rangle$ and 17% along the Fe $\langle 110 \rangle$. The strain is thus somewhat large for obtaining ideal epitaxy, but our preliminary results showed that superlattice x-ray-diffraction spectra could be attained. We therefore decided to attempt to produce a series of high-quality Fe/Pd superlattices to determine if there were significant differences in their properties from those of multilayers made with this same combination.

Because of the lattice constant and symmetry mismatch, careful structural characterization of the samples is required. Structural coherence was measured using standard θ-2θ x-ray diffraction and the epitaxial orientation was inferred from wide-film Debye-Scherrer patterns. Low-angle x-ray diffraction permitted the measurement of the superlattice periodicity for short wavelengths. The chemical composition of selected samples was determined by Rutherford backscattering spectroscopy (RBS).

Transport properties are also indicators of structural perfection. Scattering from structural and chemical impurities leads to a temperature-independent resistivity, the residual resistivity. Spin waves in a solid are subject to electron scattering. It can be shown that this scattering contributes a T^2 dependence to the electrical resistivity.[12] In transition metals, *s-d* electron-electron scattering also leads to a T^2 resistance dependence.[12] Kondo explained a $\ln(T)$ variation in the resistivity of some dilute magnetic and nonmagnetic alloys in terms of an *s-d* exchange interaction.[13]

TABLE I. Parameters of the Fe/Pd Mössbauer samples.

Sample	Modulation wavelength (Å)	Total bilayers (N)	$n_{Fe}=n_{Pd}$	Total Fe thickness (Å)
A	4.2	244	1	1020
B	8.4	156	2	1310
C	14.0	156	3	2200
D	28.2	78	6	2200
E	33.2	90	8	2990
F	42.0	90	10	3800
G	46.2	90	11	4160
H	71.7	70	17	5020
I	77.8	70	18	5450
J	86.6	70	20	6070
K	188.4	49	44	9230

II. EXPERIMENTAL PROCEDURE

A. Sample preparation and characterization

The Fe and Pd were deposited by magnetically enhanced dc sputtering guns. The sputtering system has been described elsewhere,[14] as has our technique for growing several samples with different wavelengths at the same time.[15] With all relevant deposition parameters held constant (Ar pressure, plasma current and voltage, target current, and substrate table velocity), deposition rates were constant to better than ±0.3%. Typical deposition pressures were in the range 4–6 mTorr during sputtering, and on the order of 5×10^{-8} Torr immediately before and after sputtering.

The calibrations of the deposition rates from the Fe and Pd targets were done by sputtering onto masked glass substrates for a fixed time under identical conditions as used for a superlattice deposition. An optical interferometer was used to obtain a direct measurement of the total thickness of these films, from which the rate could then be accurately determined. We used a set of graphite and sapphire [1120] substrates for each deposition, as explained in the next paragraph. The cleaning procedure we used depends on the type of substrate chosen for the deposition. The depositions were made at room temperature with both equal and unequal numbers of atomic layers n of Fe and Pd in each bilayer Λ. Table I lists the samples produced for the Mössbauer studies.

We used RBS to verify the ratios of the nominal constituents of our samples, as well as to estimate the impurity levels. Identically prepared samples on carbon substrates were used for the latter, backscattering from the normal sapphire (Al_2O_3) substrates would completely oblitrate signals from low-Z impurities. For example, Fig. 1 shows RBS data for 70 bilayers of 20 Å of Fe and 41 Å of Pd (total thickness 4270 Å) on a carbon substrate. The incident $^4He^+$ ion beam was at 4.7 MeV and the laboratory backscattering angle was 170°. The RBS depth resolution for these conditions is ±150 Å so the individual layers cannot be seen in this spectrum.

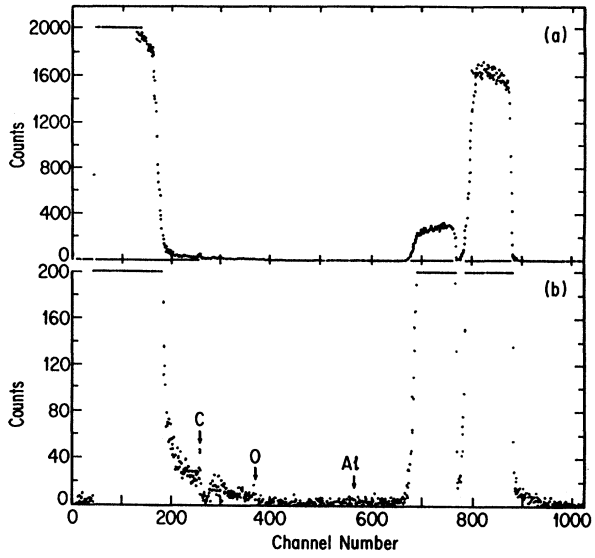

FIG. 1. Backscattered spectra of $^4He^+$ at 4.7 MeV from a 3000-Å thick Fe/Pd superlattice on a carbon substrate. (a) Total backscattered spectrum for FePd multilayer, (b) same as (a), but with 10× expanded intensity scale.

The Pd peak is at the far right (high-energy) end and its right edge corresponds to the energy of $^4He^+$ ions backscattered from the sample's surface. At this high energy, the Fe and Pd peaks are resolved, so their areal densities, listed in Table II, are obtained with an accuracy of better than 3%. (It takes several runs at different energies to resolve the peaks when they overlap if such high accuracy is required.[16]) The positions of the peaks for $_8$O and $_{13}$Al (sapphire) are indicated. None are visible, so the values listed in Table II represent an upper limit consistent with the background level. RBS detection sensitivity is $\propto Z^2$, so these values are indicative of the detection limits for the elements from $Z=6$ to ~15. The small peak labeled C is carbon on the sample's surface. The carbon substrate peak is to the far left. There is usually a tail on this peak so it is possible to say only that the carbon level in the sample is 1±1 at %.

Wide-film Debye-Scherrer (Read) camera x-ray-diffraction patterns of the samples were taken with Cu $K\alpha$ radiation.[17] This technique gives a qualitative picture of the structure of our superlattices. The incident beam was

TABLE II. RBS results from Fig. 1. See Sec. II A for interpretation of results.

Element	Fe	Pd	Ar	Al	O
Areal Density ($\times10^7$ atoms/cm^2)	22.8±0.7	12.5±0.4		<0.9	<2.5

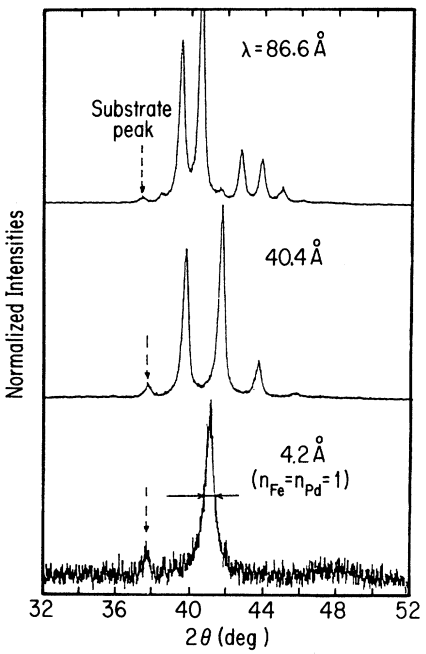

FIG. 2. θ-2θ x-ray-diffraction spectra of three Fe/Pd samples. The lowest curve is for a sample consisting of one atomic layer each of Fe and Pd. Note the narrow linewidth of the diffraction peak.

kept at an angle of 18° with respect to the plane of the substrate for all patterns so direct comparisons could be made. We find the samples to be polycrystalline, but with a high degree of texturing.

Quantitative values for the grain size and the modulation wavelength were obtained from analysis of standard θ-2θ Bragg diffraction at high angles.[18] The grain size was determined by deconvoluting the instrumental profile from the superlattice peaks using a fast Fourier transform (FFT) program[19] and applying Scherrer's equation to the linewidth of the deconvoluted peak. The modulation wavelength also can be directly determined from the angular spacing of adjacent satellites in θ-2θ x-ray scans. In Fig. 2 we show high-angle scans of several samples.

B. Mössbauer analysis

The samples formed the back wall of a 2π conversion electron detector. The source was 25 mCi of ^{57}Co in Rh. The flow gas was a He–5% CH_4 mixture. Data were collected both in constant acceleration sawtooth (flyback) and triangular wave modes. Frequent calibrations using natural iron foils were made. The full width at half maximum for the natural iron in our spectrometer was 0.26 mm/s. The system maintained this linewidth on a 4 day stability test.

Data were analyzed by least-squares fitting[20] with one or two sets of six-line hyperfine Lorentzians. Widths and areas could be constrained as desired. Spectra with broadened lines also were fitted by Window's Fourier deconvolution program.[21] Both methods gave consistent results.

C. Electrical resistivity

Samples were cooled by a CTI closed-cyle refrigerator and controlled to better than 1% over the entire temperature range from 7.5 to 300 K. Silicone vacuum grease was used to establish thermal contact between the sample holder and samples. Indium solder was used to attach copper leads for four-terminal resistance measurements. Data were acquired and digitized using a $6\frac{1}{2}$-digit voltmeter and stored in computer memory for later analysis.

The van der Pauw method[22] was used to measure the resistivity. The uncertainties in the calculations of resistivity were determined as described in the van der Pauw paper.

III. EXPERIMENTAL RESULTS

A. Structure

The RBS data in Table II give the areal density of each atomic species averaged over the entire thickness of the

TABLE III. Grain sizes for Fe/Pd superlattices.

Mössbauer sample	n_{Fe}/n_{Pd}	FWHM (deg) measured	FWHM (deg) corrected	Angle (deg)	Grain size (Å)
A	1/1	0.417	0.385	20.59	218
B	2/2	0.500	0.474	20.59	166
	4/4	0.520	0.495	20.65	170
	8/8	0.583	0.561	20.71	150
G	11/11	0.417	0.385	20.83	219
	15/15	0.625	0.604	20.15	139
J	20/20	0.333	0.292	20.35	287
	15/1	0.833	0.818	21.83	104
	18/2	0.667	0.647	21.75	131
	20/4	0.667	0.647	21.85	131
	18/13	0.562	0.539	20.71	156
	20/15	0.563	0.539	21.79	157
	22/16	0.667	0.647	20.50	131

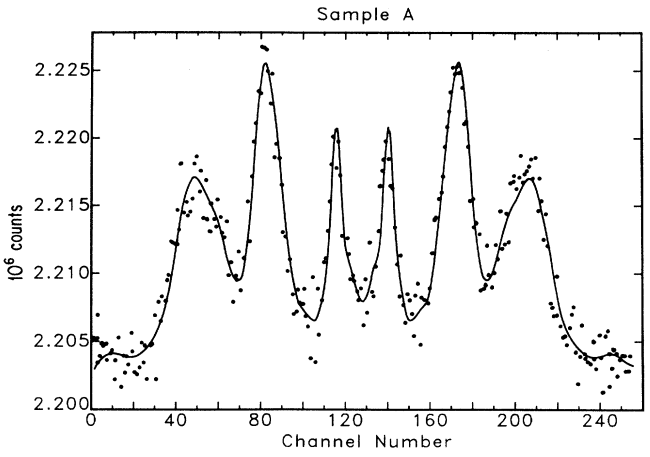

FIG. 3. Mössbauer velocity spectrum from sample A. Channel number corresponds to velocity. The solid line is a least-squares fit using Window's Fourier deconvolution method (Ref. 21).

sample. These areal density values can be converted to film thicknesses if the densities are known. Although RBS gives accurate Fe/Pd ratios for the entire sample, the detector used at these energies has insufficient energy resolution to allow resolving the individual layers. Thus, the x-ray results must be used for a structural characterization. The structural orientation of the Fe was found to be [110] perpendicular to the plane of the substrate and Pd [111].

The Bragg-Brentano θ-2θ x-ray-diffraction data for the sample consisting of $n=8$ layers each of Fe and Pd were analyzed in detail using Guinier's method. Tabulated values for form factors corrected for the measured peak-integrated intensity and position were used in the analysis.[23] These results allowed us to put an upper limit of 3 atomic layers for the amount of interdiffusion at the interfaces. This is an upper limit because of experimental limitations in detecting higher-order satellite peaks which have intensities below the diffractometer noise level.

Table III lists the results for the FFT analyses of the structure of the samples used for these studies. The grain size tends to be larger when the atomic concentrations of Fe and Pd are equal. The mosaic spread was found to be relatively narrow.

B. Mössbauer effect

Figure 3 shows the Mössbauer velocity spectrum fitted to the data for sample A ($n_{\mathrm{Fe}}=n_{\mathrm{Pd}}=1$) by Window's technique. Figure 4 shows the hyperfine-field distributions $P(H)$ derived from the velocity spectra for samples $A-D$. Note that $P(H)$ for sample A is very broad and featureless. This indicates that the Fe nuclei experience H_{hf} values which are distributed randomly about the peak value of approximately 320 kG. At $n=2$, a shoulder appears, hinting a peak at $\approx$250 kG. As n is increased, this shoulder continues to grow and become more distinct. By sample D, $n=6$, the 250-kG peak is well resolved, but small. For $n \geq 10$, this peak is lost in the background and the velocity spectrum is much sharper, approaching that of bulk Fe.

The main peak, with the exception of the $n=1$ sample, occurs at higher-field values than for bulk iron at room temperature (330 kG). This is true for samples up to about $n=18$. The main peak also is much broader than

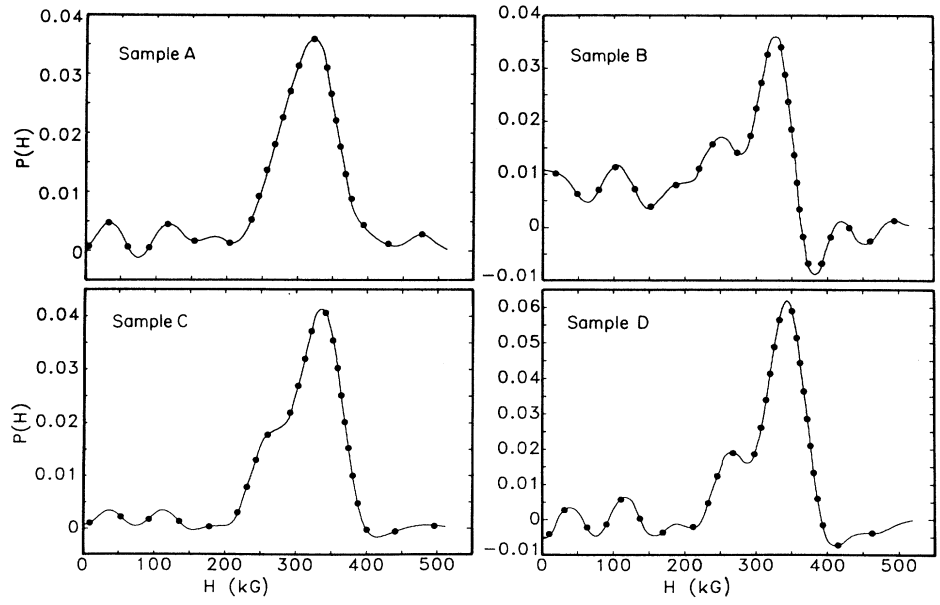

FIG. 4. The hyperfine-field distribution $P(H)$ vs H as determined by the Fourier deconvolution of the velocity spectrum for Mössbauer samples $A-D$.

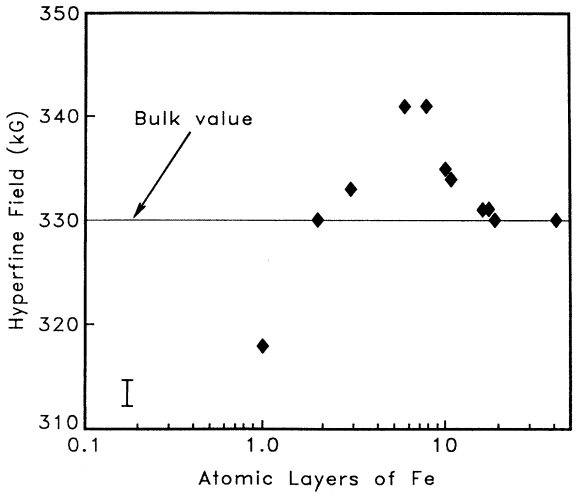

FIG. 5. Mean hyperfine field H_{hf} for samples $A-J$ as a function of number of atomic layers n. Experimental uncertainty in H_{hf} is indicated by the bar in the lower left corner.

the natural linewidth, indicating a range of local field values. Fits using two sets of hyperfine lines were made to give an idea of the relative amounts of iron in high-field and low-field environments. As could be expected, these fits had much better values of χ^2 than a single six-line fit. They also had narrower linewidths, but still several times natural. The major conclusions were identical from the six-line and the two six-line fits. Specifically, both methods gave optimum fits for intensity ratios of 3:4:1 with the exception of $n=1$, for which the best fit was 3:3:1. This indicates that, for all but the smallest Λ, H_{hf} lies in the plane of the film. For $n=1$, it is rotated slightly out. Figure 5 shows the average H_{hf} for samples with $n=1-20$ listed in Table I.

The isomer shifts relative to pure Fe for $n \geq 10$ (i.e., $n \geq 42.0$ Å) are smaller than our experimental error of ± 0.02 mm/s. Our technique did not permit an accurate measurement for samples with smaller Λ. There was no sign of a paramagnetic peak for any of the samples tested. Likewise, no significant quadrupole effects were detected.

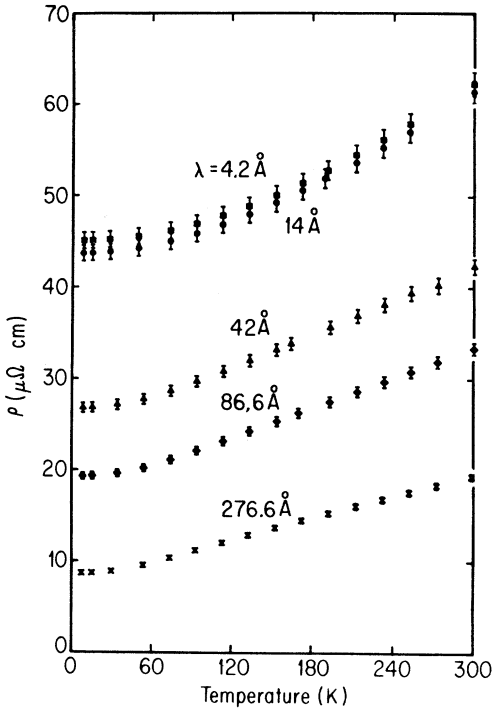

FIG. 6. Measured in-plane electrical resistivity ρ vs temperature for five Fe/Pd superlattices.

C. Electrical resistivity

Figure 6 shows the temperature dependence of the in-plane electrical resistivity of five samples. To see if the *s-d* exchange scattering was important, the data were fitted with two phenomenological equations:

$$\rho(T)=\rho_0+aT^2 \tag{1}$$

and

$$\rho(T)=\rho_0+aT^2+b\ln(T)\ , \tag{2}$$

where ρ_0, a, and b are the fitting parameters. Table IV gives the results along with pertinent properties of the

TABLE IV. Values for two- and three-parameter least-square fits to Fe/Pd electrical resistivity.

Mössbauer sample	Λ (Å)	$n_{Fe}=n_{Pd}$	Total bilayers	Total thickness (Å)	ρ_0 ($\mu\Omega$ cm)	a (Ω cm K$^{-2}\times 10^{-11}$)	b [$\mu\Omega$ cm(lnK)$^{-1}$]	χ^2
	276.6	66	11	3040	9.13	14.0		22.2
					6.80	10.9	0.718	9.67
J	86.6	20	70	6070	20.00	17.3		4.85
					16.80	13.9	0.924	1.92
F	42.0	10	90	3800	27.70	18.5		2.48
					24.10	15.2	0.984	1.01
C	14.0	3	156	2200	44.00	20.7		0.19
					42.60	19.3	0.390	0.10
A	4.2	1	244	1020	45.20	19.9		0.06
					44.50	19.2	0.202	0.04

samples. Inclusion of the logarithmic term always improved the goodness of the fit.

IV. DISCUSSION

The increased H_{hf} in Fe/Pd superlattices can be explained by the well-known giant moment of Pd. This results in an increased moment on the Fe when there is an appropriate number of Pd neighbors. Zhang *et al.*[24] have determined H_{hf} for nonequilibrium vapor-quenched $Fe_{1-x}Pd_x$ alloys. They find values above bulk Fe for alloys with concentrations in the range $0<x<0.4$. Similar results were found by Klimars *et al.*[25] for alloys made by diffusing Fe into Pd foils. The most obvious explanation, then, for an increased H_{hf} is that some interdiffusion at the interfaces between the layers has occurred. To further verify this explanation would require measurements at a synchrotron source, where the inceased x-ray intensity would allow many more x-ray superlattice lines than can be obtained from a sealed-tube source. These data could then be deconvoluted as discussed in Sec. III A to obtain a more accurate value on the amount of interdiffusion.

Jaggi *et al.*[26] have observed a similar Mössbauer line broadening in Fe/V superlattices, but with a component of H_{hf} lower than bulk. They quite accurately fitted their own data and predicted the spectra for other[27] samples with an Additive Hyperfine Interaction Perturbation (AHIP) model. We used a model in the same spirit, but much simpler, more like that of Bayreuther.[1] Diffusion of either two or three atomic layers was assumed. For the two-layer case, Jaggi *et al.*'s composition profile,[26] inferred from their Fe/V Mössbauer data, was obtained for our model by scaling from their graph. Starting from within a layer and proceeding toward the interface gave Fe concentrations starting at 100% and decreasing to 96, 75, 25, and 4% in each atomic plane as the interface region is traversed. For three layers, values of 96, 85, 65, 35, and 4% were used. Values of H_{hf} obtained from data on FePd alloys of these compositions were scaled from the data reported by Klimers *et al.*[25] The resulting values were reduced by 10 kOe to compensate for the fact that these data were for 20 K whereas ours were room-temperature measurements. A mean field was then calculated, weighted by the fraction of Fe having a given H_{hf}. The experimental value for the mean field was obtained by fitting a single six-line pattern to the data and the results are plotted in Fig. 5. For $8<n<20$, the calculated and experimental values agreed within ± 2 kG. The model was too simple for the lower-n samples. The experimental results are consistent with a reduced H_{hf} at the interface Fe layer. For intermediate n, the influence of the giant moment of Pd on the interdiffused Fe is readily apparent. By $n=20$, the bulk H_{hf} is reached.

Because H_{hf} is relatively independent of concentration for Fe $\geq 60\%$, reasonable changes in the diffusion profile do not make significant changes in the calculated results. Certainly these changes would be less than might be expected due to the lattice-mismatch strain. In Pd and some other materials, shear and tetragonal distortion have produced quite large changes in the magnetization.[26] Also, in this range of Fe $\geq 60\%$, the crystal structure of Fe-Pd changes from fcc to body-centerd tetragonal to bcc with almost no change in H_{hf}.[25]

That structural changes will affect H_{hf} is more apparent on the low Fe concentration side. The Klimers *et al.* data do not show as rapid a decrease in H_{hf} with x as those of Zhang *et al.* The latter report $H_{hf}=250$ kG at $x\cong 0.65$, whereas an extrapolation of the former gives a value >250 kG at $x=1$. Thus, the 250-kG peak for $2\leq n\leq 8$ could be explained by a relatively uniform concentration of Fe on the Pd plane adjacent to the boundary. Since the actual Fe concentration yielding a given H_{hf} is so sensitive to structure, we can only infer that, if there is such a uniform concentration, its value would have to be $<40\%$ (i.e., $x>0.6$) to be consistent with our data.

Zhang *et al.* also found in their alloys that there was a paramagnetic component which began at $x=0.6$ and became dominant for $x>0.85$. No sign of a paramagnetic peak was evident in any of our Mössbauer spectra.

The conclusion of this discussion so far is that we can explain the results by assuming interdiffusion at the interface of only two or three atomic layes: there is no need to invoke superlattice effects. However, these experimental results alone cannot rule out the possibility that there is less diffusion and that lattice strain is responsible for some of the broadening.[28]

Light scattering experiments[29] from some of the same samples used for the present work showed sharp peaks in the Brillouin scattering spectra that were consistent with interdiffusion of only a few atomic layers. These same experiments also yielded a mean magnetization M of the Fe layers. It was found that for thick Fe, M was slightly less than bulk and that, as the thickness of the Fe layers decreased, M decreased. However, as mentioned earlier, a direct proportionality between M and H can be assumed only in bulk samples. Until a detailed calculation is done, these light scattering results cannot be simply interpreted as directly confirming the Mössbauer results.

Structural properties of the samples also explain some of the electrical behavior. The residual resistivity ρ_0 (Table IV) increased when the superlattice wavelength decreased. This is consistent with the number of crystal imperfections increasing as Λ decreases. This is connected with the fact that, as Λ decreases, the total number of bilayers (and thus interfaces) increases when the total thickness is more or less the same.

The fit parameter "a" in Eqs. (1) and (2) for all samples is approximately the same as bulk values, which are 13 and 33 (10^{-11} $\Omega\,\mathrm{cm}\,K^{-2}$) for Fe and Pd, respectively. The increase of a as Λ decreases is explained by the number of spin excitations and charge fluctuations increasing when Λ decreases.

The improved fit with the inclusion of the logarithmic term in Eq. (2) is consistent with the s-d exchange interaction being significant in these materials. The parameter b decreases as Λ decreases, so that, for this system, other mechanisms become more important when the structural disorder is larger. We have found that, for Fe/W, the reverse is true: the logarithmic term dominates for the monolayer superlattice.[30]

In summary, a series of Fe/Pd superlattices of varying numbers of atoms per layer n were fabricated and studied. Superlattice lines were present in the x-ray-diffraction spectra for all Fe/Pd samples including $n=1$. Our x-ray characterization showed that all samples were polycrystalline, but textured, with a larger grain size when the atomic concentrations of Fe and Pd were equal. The x-ray spectra are consistent with an upper limit for interatomic diffusion at the interfaces of three atomic layers. Mössbauer spectra, interpreted by a simple model, were also consistent with diffusion of two or three layers, although lattice mismatch strains also could have been responsible for some of the line broadening. No electronic or magnetic superlattice effects were required to explain the results.

The presence of a low-field peak in $P(H)$ for $n \leq 10$ is consistent with the earlier observation that the first atomic layer of Fe in contact with Pd has a lower than bulk H_{hf}. This is not surprising, since this interface region becomes a larger fraction of the sample as n becomes smaller. However, no paramagnetism (or superparamagnetism) at the level of 1% of the sample was observed.

The electrical resistivity results also were consistent with the structural characterizations. The *s-d* exchange interaction was found to be significant for all Λ, but its importance decreased as Λ decreased owing to the increasing numbers of structural imperfections.

ACKNOWLEDGMENTS

This research was supported by the Office of Basic Energy Sciences, U.S. Department of Energy under Contract No. DE-FG02-87ER45297. We gratefully acknowledge Professor J. Leavitt and Professor L. McIntyre for the RBS data on our samples.

[1]G. Bayreuther, J. Magn. Magn. Mater. **38**, 273 (1983).
[2]W. Keune, Hyperfine Interact. **27**, 111 (1986).
[3]Charles M. Falco, in *Physical Fabrication and Applications of Multilayerd Structures,* edited by P. Dhez (Plenum, New York, 1988), Chap. 1.
[4]C. S. Wang and A. J. Freeman, Phys. Rev. B **24**, 4364 (1981).
[5]S. Ohnishi, A. J. Freeman, and M. Weinert, Phys. Rev. B **28**, 6741 (1983).
[6]N. K. Jaggi and L. H. Schwartz, J. Phys. Soc. Jpn. **54**, 1652 (1985).
[7]U. Gonser and H. G. Wagner, Hyperfine Interact. **24-26**, 769 (1985).
[8]T. Shinjo, in *Metallic Superlattices,* edited by T. Shinjo and T. Takada (Elsevier, Amsterdam, 1987), p. 107.
[9]J. Tyson, A. H. Owens, J. C. Walker, and G. Bayreuther, J. Appl. Phys. **52**, 2487 (1981).
[10]T. Shinjo, N. Hosoito, K. Kawaguchi, N. Nakayama, T. Takada, and Y. Endoh, J. Magn. Magn. Mater. **54-57**, 737 (1986), and references cited therein.
[11]N. Hosoito, T. Shinjo, and T. Takada, J. Phys. Soc. Jpn. **50**, 1903 (1981).
[12]Paul L. Rossiter, *The Electrical Resistivity of Metals and Alloys* (Cambridge, London, 1987), Chap. 7, and references cited therein.
[13]J. Kondo, Prog. Theor. Phys. **32**, 37 (1964).
[14]C. M. Falco, J. Phys. (Paris) Colloq. **45**, C5-499 (1984).
[15]A. Boufelfel, B. Hillebrands, G. I. Stegeman, and C. M. Falco, Solid State Commun. **68**, 201 (1988).
[16]J. A. Leavitt, P. Stoss, C. R. Edelman, R. E. Davis, S. Guttierrez, N. J. Jubb, and T. M. Reith, Nucl. Instrum. Methods B **10/11**, 596 (1985).
[17]M. H. Read and D. H. Hensler, Thin Solid Films **10**, 123 (1972).
[18]See, for example, H. P. Klug and L. E. Alexander, *X-Ray Diffraction Procedures,* 2nd ed. (Wiley, New York, 1974), Chap. 9.
[19]E. Oran Brigham, *The Fast Fourier Transform* (Prentice-Hall, Englewood Cliffs, NJ, 1974).
[20]B. L. Chrisman and T. A. Tomulillo (unpublished); Comput. Phys. Commun. **2**, 322 (1971).
[21]B. Window, J. Phys. E **4**, 401 (1971).
[22]L. L. van der Pauw, Rev. Sci. Instrum. **31**, 1189 (1960).
[23]D. B. McWhan, in *Synthetic Modulated Structures,* edited by L. Chang and B. C. Giesen (Academic, New York, 1985).
[24]S. L. Zhang, K. Sumiyama, and Y. Nakamura, J. Magn. Magn. Mater. **73**, 58 (1988).
[25]S. Klimars, J. Hesse, and B. Huck, J. Magn. Magn. Mater. **51**, 183 (1985).
[26]N. K. Jaggi, L. H. Schwartz, H. K. Wong, and J. B. Ketterson, J. Magn. Magn. Mater. **49**, 1 (1985).
[27]T. Shinjo, N. Hosoito, K. Kawaguchi, T. Takada, and Y. Endoh, J. Phys. (Paris) Colloq. **45**, C5-361 (1984); T. Shinjo, Hyperfine Interact. **27**, 193 (1986).
[28]A. J. Freeman, J. Xu, and T. Jarlborg, J. Magn. Magn. Mater. **31-34**, 909 (1983).
[29]B. Hillebrands, P. Baumgart, R. Mock, G. Güntherodt, A. Boufelfel, and Charles M. Falco, Phys. Rev. B **34**, 9000 (1986).
[30]A. Boufelfel, R. Emrick, and C. M. Falco (unpublished).